Tectonic evolution of the 'Liguride' accretionary wedge in the Cilento area; southern Italy: a record of early Apennine geodynamics

S. Vitale, S. Ciarcia, S. Mazzoli, M.N. Zaghloul

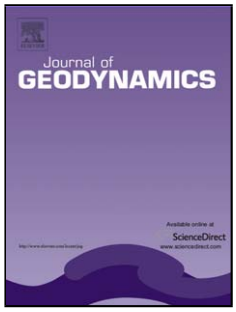

Title: Tectonic evolution of the 'Liguride' accretionary wedge in the Cilento area; southern Italy: a record of early Apennine geodynamics

Authors: S. Vitale, S. Ciarcia, S. Mazzoli, M.N. Zaghloul

PII: S0264-3707(10)00094-3
DOI: doi:10.1016/j.jog.2010.06.002
Reference: GEOD 1010

To appear in: *Journal of Geodynamics*

Received date: 8-1-2010
Revised date: 25-5-2010
Accepted date: 6-6-2010

Please cite this article as: Vitale, S., Ciarcia, S., Mazzoli, S., Zaghloul, M.N., Tectonic evolution of the 'Liguride' accretionary wedge in the Cilento area; southern Italy: a record of early Apennine geodynamics, *Journal of Geodynamics* (2008), doi:10.1016/j.jog.2010.06.002

Tectonic evolution of the 'Liguride' accretionary wedge in the Cilento area, southern Italy: a record of early Apennine geodynamics

Vitale S.[1]*, Ciarcia S. [1], Mazzoli S.[1], Zaghloul M.N.[2]

[1]Dipartimento Scienze della Terra, Università di Napoli Federico II, Largo San Marcellino 10, 80138 Napoli, Italy

[2] Department of Earth Sciences, University of Abdelmalek Essaadi, Tangier, Morocco

Key-words: subduction, superposed folding, synorogenic sedimentation, stratigraphic record, structural analysis, Apennine Orogen

* Corresponding author.

E-mail address: stefano.vitale@unina.it (S. Vitale)

Abstract

The early stages of southern Apennine development have been unraveled by integrating the available stratigraphic record provided by synorogenic strata (of both foredeep and wedge-top basin environments) with new structural data on the Liguride accretionary wedge cropping out in the Cilento area, southern Italy. Our results indicate that the final oceanic subduction stages and early deformation of the distal part of the Apulian continental margin were controlled by dominant NW-SE shortening. Early Miocene subduction-accretion, subsequent wedge emplacement on top of the Apulian continental margin and onset of footwall imbrication involving detached Apulian continental margin carbonate successions were followed by extensional deformation of the previously 'obducted' accretionary wedge. Wedge thinning also enhanced the development of accommodation space, filled by the dominantly siliciclastic Cilento Group deposits. The accretionary wedge units and the unconformably overlying wedge-top basin sediments experienced renewed NW-SE shortening immediately following the deposition of the Cilento Group (reaching the early Tortonian), confirming that the preceding wedge thinning represented an episode of synorogenic extension occurring within the general framework of NW-SE convergence. The documented Early to the Late Miocene steps of southern Apennine development are clearly distinct with respect to the subsequent (late Tortonian-Quaternary) stages of fold and thrust belt evolution coeval with Tyrrhenian back-arc extension, which were characterized by NE-directed thrusting in the southern Apennines.

1 1. Introduction

The southern Apennines are part of the peri-Mediterranean Alpine belt and result from the interaction between the converging Apulian and European plates since Late Cretaceous time (e.g. Mazzoli and Helman, 1994, and references therein). The related tectonic evolution involved the subduction of Tethyan oceanic lithosphere beneath the overriding Calabrian continental crust (Bonardi et al., 2001). Following Early Miocene docking of the two continental margins, the subduction of oceanic lithosphere gave way to that of continental lithosphere (Ranalli et al., 2000), which is also evinced by exhumed HP-LT rocks originally belonging to the distal part of the Apulian continental palaeomargin (Iannace et al., 2007). During the Early Miocene, the tectonic wedge formed by oceanic and transitional units (Liguride Units; Bonardi et al., 1988; 'Internal' Units, Ciarcia et al., 2009; Vitale et al., 2010) overthrusted the inner sector of the Apennine Platform (Mostardini and Merlini, 1986; Fig. 1). Subsequently, detached Mesozoic-Neogene sedimentary successions of the foreland (i.e. Apulian) plate were piled up eastward onto progressively outer domains, while sedimentation was occurring in both wedge-top and foredeep basins (Bonardi et al., 2009). Remnants of the oldest part of the Apennine accretionary wedge, represented by the Liguride Units and associated Miocene wedge-top basin deposits, crop out extensively in the southern Apennines (Fig. 1). The aim of this paper is to analyze the structural setting and the tectonic evolution of the Liguride accretionary wedge, in order to investigate the first steps of the Apennine orogeny. A complete structural analysis is provided for the Liguride Units and associated wedge-top basin successions cropping out in Cilento (Fig. 1).

2 2. Geological setting

The Liguride Units of the southern Apennines (Fig. 2) encompass the ophiolite-bearing Frido and Nord-Calabrese units (Bonardi et al., 1988, 2001) as well as the Parasicilide and Sicilide units (Ciarcia et al., 2009; Vitale et al., 2010, and references therein), the latter two including basin successions probably deposited on thinned continental/transitional crust. Starting from the Early Miocene, all of these units were deformed and accreted into the Apennine tectonic wedge (Ciarcia et al., 2009; Vitale et al., 2010) and then unconformably overlain by wedge-top basin deposits of the Cilento Group (Amore et al., 1988) and Monte Pruno Fm (Ciarcia et al., 2009). In the Cilento, only the Parasicilide and Nord-Calabrese units crop out (Fig. 3a). The 'Internal' Units (i.e. the Liguride Units) tectonically overlie the 'External' Units that were derived from the deformation of sedimentary cover successions belonging to the Apulian continental margin (Fig. 3a). These comprise shallow-water and slope carbonates (Apennine Platform) and pelagic basin (Lagonegro Basin) successions (e.g. Mazzoli et al., 2008, and references therein). Lower-Middle and Upper Miocene wedge-top basin deposits occur on top of the tectonic pile (Fig. 2).

The Nord-Calabrese Unit includes Jurassic pillow lavas at the base, overlain by the Timpa delle Murge Fm (consisting of argillites, quartz-arenites, limestones and jaspers) and then by the Crete Nere and Saraceno fms. In the Cilento area, only the latter two formations occur. The Crete Nere and Saraceno fms (Fig. 4) comprise a predominately siliciclastic and calciclastic succession deposited on oceanic crust (Bonardi et al., 1988) during plate convergence. The Crete Nere Fm is formed, from bottom to top, by a thick succession of black shales with intercalation of arenites, dark-brownish argillites and arenites in the middle part, and calcareous beds in the upper part. The middle-upper part of this formation has been dated as Middle Eocene; however the undated lower part could be as old as Late Jurassic, as suggested by Bonardi et al. (1988). The Crete Nere Fm stratigraphically passes

upwards to the Saraceno Fm, which is characterized by calciclastic, locally silicified turbidites (Punta Telegrafo Member) at the base, followed by marls, pelites and arenites in the middle part and finally by sandstones of the Sovereto Member (Bonardi et al., 2009). The uppermost part of the Saraceno Fm has been dated as Aquitanian-Burdigalian (Bonardi et al., 2009).

The Parasicilide Unit (Bonardi et al., 2004; Ciarcia et al., 2009; Vitale et al., 2010) cropping out in Cilento and corresponding to the Castelnuovo Cilento Unit of Cammarosano et al. (2000, 2004), comprises both pre-orogenic and foredeep basin deposits (Fig. 4) grouped into four formations (from bottom to top): (i) micaceous sandstones, varicolored clays and slates of the Postiglione Fm; (ii) marls and limestones of the Monte Sant'Arcangelo Fm; (iii) whitish marls and marly limestones of the Contursi Fm; and (iv) foredeep sandstones of the Arenarie di Albanella Fm (Donzelli and Crescenti, 1962). Due to intense folding, the original thickness of the whole succession can only be approximately estimated as exceeding 800-1000 meters. The dated portions of the succession range in age between Middle Eocene and Burdigalian; however, the lower undated deposits could be as old as Late Cretaceous (Bonardi et al., 1988; Guerrera et al., 2005).

The Cilento Group, whose age ranges from the Burdigalian/Langhian boundary (Amore et al., 1988) to the lower Tortonian (Russo et al., 1995), is formed by arenitic and marly deposits (Fig. 4) of the Pollica and San Mauro fms (Ietto et al., 1965) laterally passing southward to conglomeratic, arenitic and marly deposits of the Torrente Bruca Fm (Amore et al., 1988). The Pollica Fm is formed by a thin-bedded succession of sandstones and pelites in the lower part (Cannicchio Sandstones Member), passing to a thin- to medium-bedded succession of sandstones, conglomerates, marls and pelites in the middle-upper part. The overlying San Mauro Fm is characterized by a medium- to thick-bedded succession of marls

and conglomerates. In the Lucania region, to the east, these formations correspond to the undifferentiated succession of the Albidona Fm (Selli, 1962). These deposits and the underlying units are covered unconformably by younger (Upper Miocene) coarse-grained wedge-top basin successions including: (i) the Castelvetere Fm (Pescatore et al., 1970), (ii) the Monte Sacro Fm (Selli, 1962), and (iii) the Oriolo (Selli, 1962), Serra Manganile (Ghezzi and Bayliss, 1964) and Gorgoglione (Selli, 1962) Fms, cropping out in the Sele River Valley, Cilento and Lucania, respectively (Figs. 1, 2, 3a, 4).

The Nord-Calabrese Unit is generally tectonically superposed onto the Parasicilide Unit (e.g. Alento and Lambro River Valleys, Fig. 3a). However, in the Sapri area it lies directly over the carbonates of the Apennine Platform, whereas northeastward of Cicerale-Monte Centaurino, this unit does not crop out (e.g. Torrente Pietra and Sele River Valleys Fig. 3a).

The Cilento Group unconformably covers the already deformed and imbricated Nord-Calabrese and Parasicilide units. This feature is shown in the geological map (Fig. 3a) and in cross section X-X' (Fig. 3b): the Cilento Group seals the Crete Nere and Saraceno fms (Nord-Calabrese Unit) in the Alento River Valley, west of the Lambro River and in the Sapri area, whereas it covers the Parasicilide Unit (located in the footwall to the Nord-Calabrese Unit) between Monte Sacro and Monte Centaurino and in the northeastern area, between the villages of Magliano Nuovo and Cicerale.

3 3 Structural analysis of the Nord-Calabrese Unit

3.1 3.1 Crete Nere Fm

The Crete Nere Fm is characterized by the superposition of three fold sets (F_1^{NC}, F_2^{NC} and F_3^{NC}) and associated planar and linear structures. The main foliation in pelitic layers is a slaty cleavage (S_1^{NC}) sub-parallel to F_1^{NC} fold axial planes (AP_1^{NC}), whereas in the competent arenitic beds a spaced, disjunctive cleavage is present. F_1^{NC} folds display geometries ranging from tight to isoclinal (Fig. 5a). Fold shape alternates between classes 1c and 3 of Ramsay (1967) in competent and incompetent units, respectively. F_2^{NC} folds are characterized by larger interlimb angles with respect to preexisting F_1^{NC} folds. Fold interference patterns range from perfectly coaxial (type 3; Ramsay, 1967) to moderately non-coaxial (intermediate type 2-3, Fig 5a). A crenulation cleavage (S_2^{NC}) and a crenulation lineation (L_2^{NC}) occur in the pelitic units. Bedding (S_0^{NC}) is marked by the occurrence of arenitic beds or by layers of differing composition and color in the fine-grained layers. A macro-scale fold (here termed Orria Syncline, as it is exposed around the Orria village; Fig. 3a) and related parasitic folds F_3^{NC} deform this succession in the NE sector of the study area, whereas rare meso-scale F_3^{NC} folds occur elsewhere.

Orientation data for the main structures exposed between Pisciotta Marina and Pioppi (Fig. 3a) are shown in Fig. 6. Bedding and (S_1^{NC}) foliation poles (Figs. 6a, f) form two girdles providing theoretical (π_1 and π_2) fold axes plunging 055/07 and 065/16, respectively. (The latter value, obtained from folded S_1^{NC}, is related to second-phase folds). F_1^{NC} and F_2^{NC} folds are about coaxial: mesoscopic fold hinges A_1^{NC} (Fig. 6b) show a mean plunge of 051/19 and mesoscopic fold hinges A_2^{NC} (Fig. 6g) form a cluster around the mean value of 064/12 whereas in the Pioppi area A_1^{NC} data (Fig. 6c) define a girdle. The crenulation lineation (L_2^{NC}) is parallel to A_2^{NC} fold hinges (Fig. 6h), to which is clearly related, and displays a mean plunge of 066/12. The axial planes AP_1^{NC} of F_1^{NC} folds are dipping mainly to the SE (Fig. 6d) in the Pisciotta Marina area, whereas in the Pioppi area they are scattered (Fig. 6e). The axial

planes AP_2^{NC} of F_2^{NC} folds dip both to the NW and SE in the Pisciotta Marina area (Fig. 6i). Poles to the associated crenulation cleavage (S_2^{NC}) form two clusters including both moderately SSE dipping and NNW gently dipping sets (Fig. 6j).

The third fold set (F_3^{NC}) is well-exposed in the Pioppi area. A_3^{NC} fold hinges (Fig. 6k) cluster around a mean value of 301/19, while fold axial planes are dominantly NE to SW dipping (Fig. 6l).

3.2 3.2 Saraceno Fm.

Structural analysis on the Saraceno Fm has been carried out separately for the pelitic-calcareous lower part (Punta Telegrafo Member) and for the arenitic-marly middle-upper portion. The analyzed lower part of the formation crops out at Pisciotta Marina, Punta Telegrafo and Torre di Caleo (Fig. 3a). The Punta Telegrafo Member is characterized by the superposition of two meso-scale fold sets F_1^{NC} and F_2^{NC} (Fig. 5b). F_1^{NC} folds show tight to isoclinal geometries, with shapes ranging from chevron, rounded and box types (Fig. 5b). Generally F_1^{NC} folds in pelitic rocks are of class 3 of Ramsay (1967), whereas they are of class 1c for calcareous and arenitic layers. Second-phase folds (F_2^{NC}) include open to tight folds (Fig. 5b) that are locally intensely developed (Fig. 5d). Variably developed cleavages are associated with the two fold sets. In the pelites, the first foliation (S_1^{NC}) is a roughly axial planar slaty cleavage (involving total or partial transposition), whereas the second foliation (S_2^{NC}) is a crenulation cleavage (Fig. 5c) to which a crenulation lineation (L_2^{NC}) is also associated. Late, open F_3^{NC} folds refold this part of succession.

Complex vein arrays affect the whole calcareous succession, especially at Punta Telegrafo site (Fig. 5f). Most of the veins are orthogonal to F_1^{NC} fold hinges or form conjugate sets,

183 often in the form of en-echelon vein arrays, both indicating extension parallel to the fold axis
184 A_1^{NC}. Veins parallel to A_1^{NC} also occur, producing a characteristic chocolate tablet boudinage
185 (Fig. 5f). Locally, especially in the isoclinal fold limbs, intense stretching occurs in the form of
186 conjugate ductile shear zones (Fig. 5e) or as asymmetric boudinage (Fig. 5g). Extension veins
187 orthogonal to F_2^{NC} fold hinges also occur, although they are less common. For both folding
188 events, fold amplification was preceded by homogeneous shortening (bedding-parallel
189 shortening for the first event), expressed by local thrust faults characterized by minor
190 displacements (pre-buckle thrusts; Price and Cosgrove, 1990). Often the second shortening
191 affects previously boudinaged layers (Fig. 5h). The interference pattern developed by the
192 superposition of F_1^{NC} and F_2^{NC} fold sets is of intermediate 2-3 type of Ramsay's (1967)
193 classification (Fig. 5b), F_2^{NC} fold hinges forming a generally low angle with F_1^{NC} fold axes.
194 Nearly coaxial refolding is recorded by the distribution of bedding attitudes, the composite
195 structures resulting from fold superposition maintaining an overall sub-cylindrical geometry.
196 Poles to S_0^{NC} form girdles (Fig. 7a, b) indicating theoretical (π_1) fold axes of 064/09 (Punta
197 Telegrafo) and 231/21 (Torre di Caleo). Poles to S_1^{NC} (Fig. 7g) are also distributed around a
198 great circle whose pole plunges 237/06, this value representing the theoretical (π_2) fold axis
199 for the second-phase fold set. First-phase fold hinges (A_1^{NC}) are scattered (Fig. 7c, e).
200 However, the related axial planes (AP_1^{NC}) dip mainly to the NW and SE (Fig. 7d, f).
201 Conversely, second-phase fold hinges (A_2^{NC}) form a subhorizontal cluster (Fig. 7h, k, m) with
202 mean plunges of 037/06 (Pisciotta Marina), 042/00 (Punta Telegrafo) and 066/12 (Torre di
203 Caleo). The related fold axial planes (AP_2^{NC}) dip mainly to the NW and SE (Fig. 7j, l, n). A
204 crenulation cleavage (S_2^{NC}) and a crenulation lineation (L_2^{NC}) are associated with second-
205 phase folds. S_2^{NC} surfaces tend to dip either moderately to the NW or gently to the SE (Fig.
206 7o), whereas lineations L_2^{NC} form a cluster with a mean plunge of 248/04 (Fig. 7i).

The middle-upper part of the Saraceno Fm is characterized by structures similar to those described for the lower part, although F_3^{NC} folds become more abundant. As for the Punta Telegrafo Member, this part of the succession is characterized by three fold sets: F_1^{NC}, F_2^{NC} and F_3^{NC}. Generally F_1^{NC} folds are tight to isoclinal and show variable geometries with chevron to rounded shapes, whereas F_2^{NC} folds are more open (Fig. 8a, b). Poles to bedding are scattered (Fig. 7p) with dominant NW and SE dip directions. F_1^{NC} fold hinges and axial planes are also scattered (Fig. 7q, r). The related cleavage (S_1^{NC}) dips mainly to the NW and SE (Fig. 7s). F_2^{NC} fold hinges plunge mainly to the NNE and S/WSW (Fig. 7t). F_2^{NC} fold axial planes are mainly gently dipping to sub-horizontal (Fig. 7u), similarly to the related crenulation cleavage S_2^{NC} (Fig. 7v). As for the lower part of the formation, also here interference patterns between F_1^{NC} and F_2^{NC} folds are of intermediate type between types 2 and 3 of Ramsay's (1967) classification (Fig. 8a, b). F_3^{NC} folds generally display open to tight shapes, with dominantly W-E trending hinges (Fig. 7w) and axial planes dipping mainly to the S and secondarily to the N (Fig. 7x). The previously mentioned Orria Syncline, representing a regional F_3^{NC} structure, involves also the Saraceno Fm in the NE part of the study area.

4 4. Structural analysis of the Cilento Group

In order to unravel possible stratigraphic controls on structural development and to analyze the role of bed-thickness on folding style, (i) the lower part (Cannicchio Sandstones Member) of the Pollica Fm, (ii) the middle-upper part of the Pollica Fm, and (iii) the San Mauro Fm have been analyzed separately. The analyzed outcrops are localized around the Pollica, Omignano, Orria, Gioi, Salento and Catona villages (Fig. 3a).

4.1 4.1 Lower part of the Pollica Fm: Cannicchio Sandstones Member

Several outcrops of the Cannicchio Sandstones Member have been analyzed, particularly in the Cannicchio type-locality (close to the Pollica village; Fig. 3a). In this area the succession is characterized by (F_1^{CG}) folds showing kink and chevron shapes (fig 8c), and subordinate rounded or box geometries. These folds are often detached along pelitic layers (Fig. 8c) forming SE verging asymmetric fold trains characterized by overturned short limbs. It is common to find stiff beds sandwiched between pelitic layers and shortened by NW or SE dipping pre-buckle thrusts showing minor displacements (Fig. 8d). Minor thrust faults occur also in fold hinge regions to accommodate shortening in thinner layers (Fig. 8c, inset). In the Omignano area (Fig. 3a) the whole succession is deformed by a SE verging, overturned macro-scale F_1^{CG} fold and associated parasitic structures. In the area between Omignano, Pollica and Ogliastro, F_1^{CG} fold hinges of both meso- and macro-scale folds show a general NE-SW trend. A spaced, disjunctive cleavage (S_1^{CG}) is associated with these folds.

Conversely, in the Orria, Gioi and Cardile areas the whole succession of the Cilento Group is deformed by the SW-S verging regional Orria Syncline (Zuppetta and Mazzoli, 1997), which represents a F_1^{CG} structure in terms of the Cilento Group deformation.

Figure 9 (a to h) shows orientation data for the main analyzed structures. Poles of bedding form girdles (Fig. 9a-c) providing theoretical (π_1) fold axes plunging 229/06 (Cannicchio), 048/13 (Omignano) and 248/01 (Salento-Orria area). F_1^{CG} fold hinges are clustered (Fig. 9d, f) around two maxima plunging 240/31 and 047/02, whereas fold axial planes AP_1^{CG} dip mainly to the NW and SE (Fig. 9e, g). Top-to-the-NW and -SE reverse fault kinematics are compatible with NW-SE shortening (Fig. 9h).

4.2 4. 2 Middle-upper part of the Pollica Fm

Meso-scale F_1^{CG} folds are generally asymmetric and show geometries ranging from open to tight, with chevron, rounded, box and kink shapes (Fig. 8e, f). Deformation in fold hinge regions is often accommodated by thrust faults or by cataclasis producing intense brecciation (Fig. 8f). Also in this part of the succession, pre-buckle thrusts commonly affect single stiff layers (Fig. 8g, h, i). In the Omignano area (Fig. 3a) minor parasitic folds are related to the previously mentioned overturned, SE verging major F_1^{CG} fold. The middle-upper part of the Pollica Fm is also deformed by the previously mentioned regional fold and associated S-SW verging parasitic folds in the Orria-Gioi area.

Poles to bedding distributions (Fig. 9i-n) provide theoretical (π_1) fold axes plunging 068/19 (Ogliastro-Agnone), 208/22 (Pollica), 261/16 (Catona), 045/10 (Omignano), 255/02 (Orria-Piano Vetrale), and 322/03 (Gioi-Cardile). F_1^{CG} fold hinge lines (Fig. 9o, p) display mean plunges of 069/09 (Ogliastro-Agnone) and 028/10 (Omignano), whereas fold axial planes dip mainly to the SE in the Ogliastro-Agnone area (Fig. 9q) and both to SE and NW in the Omignano area (Fig. 9r).

4.3 4.3 San Mauro Fm

The San Mauro Fm crops out mainly in the N and NE sectors of the study area. In the former it shows only gentle F_1^{CG} folds, whereas in the latter it is deformed by the previously mentioned regional F_1^{CG} fold and associated open to tight parasitic folds with steep to gently dipping axial planes and fold vergence ranging between SE and SW. In this formation,

279 mesoscopic folds develop overturned limbs only locally (Cardile and Gioi villages) and display
280 larger wavelengths with respect to F_1^{CG} folds in the underlying Pollica Fm.
281 Poles to bedding (Fig. 9s-u) indicate gentle folding in the Omignano area (Fig. 9s), whereas in
282 the Orria-Piano Vetrale and Gioi-Cardile areas they form girdles (Fig. 9t, u) providing
283 theoretical (π_1) fold axes plunging 286/01 and 127/04, respectively (these being related to
284 the regional Orria Syncline). Fold hinges are scattered (Fig. 9v), whereas fold axial planes dip
285 mainly to the NNE and SSW (Fig. 9w).
286

287 ## 5 5. Discussion

288

289 The Crete Nere and Saraceno fms, forming the Nord-Calabrese Unit, show similar polyphase
290 deformation (D^{NC}_1, D^{NC}_2 and D^{NC}_3) characterized by three superposed fold sets (F_1^{NC}, F_2^{NC} and
291 F_3^{NC}). The almost coaxial geometry of the first two fold sets and the limited temporal range
292 in which they must have occurred suggests that the two folding events developed as part of
293 a progressive deformation event characterized by roughly NW-SE shortening. Initial layer-
294 parallel shortening during the D^{NC}_1 deformation stage produced mesoscopic thrust faults
295 showing minor displacements (pre-buckle thrusts). Subsequent fold amplification led to the
296 development of dominantly isoclinal folds (F_1^{NC}). This process was accompanied, especially in
297 the calcareous beds (lower part of the Saraceno Fm), by boudinage and formation of en-
298 echelon vein arrays. Boudinage is intensely developed at the transition between the Crete
299 Nere and Saraceno Fms, where the strata are often completely disrupted by conjugate
300 extensional shear zones. Widespread veining reveals significant fluid localization at this level
301 of the succession, a process probably controlled by the stratigraphic boundary between the
302 low permeable shales and slates of the Crete Nere Fm and the high permeable limestones

303 forming the lower part of the Saraceno Fm. Veins, boudins and conjugate shear zones
304 indicate extension along both the maximum (X) and intermediate (Y) axes of the bulk finite
305 strain ellipsoid (i.e. oblate strain). Furthermore the occurrence of stretched isoclinal folds
306 (intrafolial folds) and shortened boudins strengthens the hypothesis of progressive
307 deformation. The layers were first shortened (by buckling) and then, as fold limbs came to lie
308 roughly parallel to the maximum extension direction as a result of isoclinal folding, they
309 were stretched, leading to the development of intrafolial folds. Such previously lengthened
310 fold limbs, characterized by boudinage of the stiff layers, were subsequently shortened
311 (locally developing 'folded boudins'; Ramsay and Huber, 1983) during the second
312 deformation stage. This (D^{NC}_2) is characterized by tight to open (F_2^{NC}) folds, verging mainly to
313 the SE and subordinately to the NW. The almost coaxial geometry of F_1^{NC} and F_2^{NC} fold sets,
314 evident for the Crete Nere Fm and the lower part of the Saraceno Fm, is less consistent for
315 the middle-upper part of the Saraceno Fm, resulting in interference patterns ranging
316 between types 2 and 3 of Ramsay (1967). The third deformation stage (D^{NC}_3) is characterized
317 by the local development of meso- and macro-scale F_3^{NC} folds (such as in the Pisciotta-Ascea
318 and Orria areas, Fig. 3a) displaying open to tight geometries.
319 The structural evolution unraveled for the Crete Nere and Saraceno fms is comparable with
320 that of the Parasicilide Unit cropping out in Cilento and forming, together with the Nord-
321 Calabrese Unit, the Liguride Units in this area. The Parasicilide Unit, located in the footwall to
322 the Nord-Calabrese Unit, is also characterized by superposed deformations (Vitale et al.,
323 2010): F_1^{PS} isoclinal folds, related to a first deformation stage (D^{PS}_1), are refolded by close F_2^{PS}
324 folds developed in the form of a regional recumbent fold verging to the SE and associated
325 parasitic folds (D^{PS}_2). A third deformation event (D^{PS}_3) produced open F_3^{PS} folds displaying
326 horizontal axial planes, developed only in the steep to vertical F_2^{PS} limbs. The first two

deformation stages are related to the accretion of this succession into the tectonic wedge in Burdigalian time and subsequent deformation within the wedge (Vitale et al., 2010). Like the Nord-Calabrese Unit, the Parasicilide succession is also deformed, in the NE part of the study area, by the regional (F_3^{PS}) Orria Syncline.

A late, extensional origin of the contacts between the Nord-Calabrese and Parasicilide Units is suggested by the geometry of the tectonic contact in the Castelnuovo Cilento tectonic window (Fig. 3a, cross sections of Fig. 3b), which dramatically cuts all folds in both footwall and hanging-wall units (Vitale et al., 2010), as well as in the Sapri area, where the Nord-Calabrese Unit directly overlies the Apennine Platform succession with the tectonic omission of the Parasicilide Unit and part of the Crete Nere Fm. The simple restoration provided in Fig. 10 shows the proposed interpretation for the development of the present structural geometry as well as of wedge-top basin depocentres filled by the Cilento Group deposits. The horizontal extension producing the two major low-angle normal faults shown in Fig. 10 is probably associated with previous wedge overthickening, as a result of thrusting of the Nord-Calabrese Unit onto the Parasicilide Unit, as well as with large-scale warping and uplift of the wedge related to footwall imbrication within the underlying Apennine Platform shallow-water to slope carbonates (Vitale et al., 2010). Probably the accretionary wedge collapsed as it exceeded the critical taper, leading to the development of extensional detachments dipping toward the foreland. This processes, together with accretion of new material at the wedge toe, allowed the slope surface angle to decrease.

The tectonic contact between the Nord-Calabrese Unit and the Parasicilide Unit is gently folded by broad NE-SW trending antiforms, probably related to footwall imbrication as shown in the geological section X-X' in Fig. 3(b). This suggests that thrusting involving the Apennine Platform succession and wedge collapse were roughly coeval. Probably part of the

Apennine Platform succession (Monte Bulgheria; Fig. 3a) was exposed already in Middle Miocene time, feeding the Cilento Group with calcareous fine-grained sediments (San Mauro Fm). In this case, the tectonic window of Castelnuovo Cilento (Alento Valley; Fig. 3a) may be interpreted as a breached anticline related to thrusting in the underlying Apennine Platform succession.

The deformation of the Cilento Group succession, unconformably overlying the previous units, is characterized by a roughly NW-SE oriented shortening (D^{CG}_1) expressed by pre-buckle thrusts, reverse faults and asymmetric folds characterized by a main vergence toward the SE and secondarily toward the NW, S and SW. These F_1^{CG} folds generally range from tight to open and show kink geometries. Folding occurred at very low-T conditions, as evidenced by brittle deformation associated with tight folds. In the NE sector of the study area, the successions belonging to the Cilento Group and the underlying Nord-Calabrese and Parasicilide units are all deformed by the regional Orria Syncline (Fig. 3a). This major fold is accompanied by a system of S-SW overturned parasitic folds (cross section Y-Y' in Fig. 3b). The π_1-axes obtained from the poles to bedding measured in the Pollica and San Mauro Fms from different areas (Fig. 9c, m, n, t, u) point out an overall curved fold hinge for the regional fold. Statistical (π_1) fold axes plunge from 248/01 (Cannicchio Member), to 255/02 (Middle-upper part of Pollica Fm), to 286/01 (San Mauro Fm) in the Orria area, to 322/05 (Middle-upper part of Pollica Fm) and 127/04 (San Mauro Fm) in the Gioi area. According to Zuppetta and Mazzoli (1997), the general lack of cleavage development and of grain-scale deformation associated with the Orria Syncline is indicative of large-scale folding occurring in not completely lithified sediments. Based on this evidence, the authors suggested an early (syndiagenetic) origin for this fold, involving the Cilento Group sediments immediately following their deposition. Deformation involving non-completely lithified sediments within

375 the general framework of thrusting and associated non-coaxial strain may have enhanced
376 non-cylindrical folding.
377 In order to obtain a synoptic view of the fold trends in the whole study area, mesoscopic fold
378 axis trends (both for the Liguride Units and the Cilento Group) are plotted in the geological
379 map of Fig. 3a. It is worth noting that a broad homogeneity in fold axis trends exists for the
380 Liguride Units ($F^{NC}_{1\text{-}2\text{-}3}$, $F^{PS}_{1\text{-}2\text{-}3}$) and for the Cilento Group (F^{CG}_{1}). The rough coaxiality between
381 the first fold set (F^{CG}_{1}) in the Cilento Group and $F^{NC}_{1\text{-}2\text{-}3}$ and $F^{PS}_{1\text{-}2\text{-}3}$ fold sets in the Nord-
382 Calabrese and Parasicilide Units suggests a more or less constant orientation of regional
383 shortening for these deformation stages.
384 Although asymmetric folds and kinematic features associated with thrust faults indicate both
385 NW and SE vergences, it is reasonable to suppose a main SE/E tectonic transport for these
386 units according to Miocene kinematic reconstructions proposed by several authors (e.g.
387 Vignaroli et al., 2009 and references therein). This is consistent with the SE vergence of first-
388 phase isoclinal folds in the Parasicilide Unit exposed in the tectonic window of Castelnuovo
389 Cilento (Fig. 3a; Vitale et al., 2010), as well as with top-to-the-ESE kinematics unraveled by
390 Vitale and Mazzoli (2009) for carbonate thrust sheets originally forming part of the Apennine
391 Platform in the Calabria-Lucania border area (Iannace et al., 2007). Major differences in
392 deformation styles occur between the Liguride Units and the Cilento Group. The Liguride
393 Units show pervasive deformation, whereas the Cilento Group is characterized by locally
394 disharmonic folding and variable fold geometries. Increasing fold wavelength from the
395 bottom to the top of the Cilento succession is probably related to general coarsening and
396 thickening upward (from the thin strata of the Cannicchio Sandstones Member to the meter-
397 scale strata of the San Mauro Fm).

The Cilento Group was deposited on an already deformed substratum consisting of the Nord-Calabrese and Parasicilide units. Therefore, the first two deformation events involving the latter two units occurred during the Burdigalian, being bracketed by the age of the Cannicchio Member (Burdigalian-Langhian boundary) and the age of the youngest deposits (Arenarie di Albanella Fm, Burdigalian) of the Parasicilide Unit. On the other hand, as suggested by Zuppetta and Mazzoli (1997), based on the analysis of the Orria Syncline and related parasitic structures, deformation of the Cilento Group immediately postdated the deposition of the youngest strata of San Mauro Fm (lower Tortonian according to Russo et al., 1995). Deformation stages for the various analyzed successions, their interpreted correlation and chronology are summarized in Table 1.

In order to summarize the present results, a geodynamic evolutionary sketch for the southern Apennine accretionary wedge between the Aquitanian-Burdigalian boundary and the post-lower Tortonian is provided in Fig. 11. In the first stage (Fig. 11a) the Nord-Calabrese succession is covered by the foredeep deposits of the Saraceno Fm (sandstones). Subsequently, this unit is incorporated into the accretionary wedge and deformed by overall NW-SE shortening (D^{NC}_1) developing isoclinal F^{NC}_1 folds (Fig. 11b). During this stage foredeep sedimentation occurs on top of the Parasicilide domain with the deposition of the sandstones of the Arenarie di Albanella Fm. In Burdigalian time (Fig. 11c, d), the Nord-Calabrese Unit experiences continued NW-SE shortening (D^{NC}_2) and the Parasicilide Unit is accreted into the wedge with the development of F^{PS}_1 and F^{PS}_2 folds (stages D^{PS}_1 and D^{PS}_2). During the Burdigalian (Fig. 11d), the inner sector of the Apennine Platform carbonate domain is overlain by the accretionary wedge, while sedimentation of the Bifurto Fm occurs in the newly developed foredeep. Later (Fig. 11e, f), the accretionary wedge undergoes horizontal stretching and vertical shortening, probably due to previous overthickening and to

footwall imbrication in the underlying Apennine Platform carbonate succession, producing bending and uplift of the Liguride Units. Low-angle extensional detachments associated with synorogenic extension favor the development of accommodation space in wedge-top basin depocentres (Fig. 11f) that are filled by the Cilento Group deposits (Fig. 11g). Subsequent to the final (early Tortonian) deposition of San Mauro Fm, the whole tectonic pile – including the Nord-Calabrese and Parasicilide Units, as well as the Cilento Group – experiences renewed, though moderate, roughly NW-SE oriented shortening (D^{NC}_3, D^{PS}_1 and D^{CG}_1) leading to the development of scattered folds (Fig. 11h).

6 6. Conclusions

The integration of available stratigraphic information with new structural data from the various tectonic units exposed in the Cilento area of the southern Apennines has allowed a comprehensive picture of the tectonic evolution of the Liguride accretionary wedge in this area to be obtained. The documented structural data point out that final oceanic subduction stages and early involvement in the deformation of the distal part of the Apulian continental margin were characterized by a broad NW-SE shortening. This, being consistent with recent plate kinematic reconstructions for the Western Mediterranean in Early Miocene times (Schettino and Turco, 2006), is completely unrelated with NE-directed thrusting characterizing the Apennine fold and thrust belt during later (late Tortonian to Quaternary) development of the Apennine-Calabrian-Sicilian arcuate orogen and associated opening of the Tyrrhenian Sea back-arc basin (e.g. Johnston and Mazzoli, 2009, and references therein).

The progressive development of the accretionary wedge in Miocene times is marked by synorogenic sedimentation both in the trench and in wedge-top basins. Major overthrusting

of Liguride Units, wedge overthickening and subsequent emplacement ('obduction') on top of the Apulian continental palaeomargin were followed by wedge collapse. This was probably coeval with – and partly related to – incipient footwall imbrication within underlying Apennine Platform carbonates. Late deformation of the accretionary wedge, post-dating deposition of the Cilento Group wedge-top basin sediments (ending in the earliest Tortonian), was controlled by renewed more or less NW-SE oriented shortening, thus confirming that the previous wedge thinning episode took place within the general framework of plate convergence.

The results, shedding new light into the Miocene tectonic evolution of the southern Apennine accretionary wedge, provide new insights into the early stages of southern Apennines development. This will hopefully contribute to a better understanding of a critical stage of Apennine geodynamics, involving the transition from the subduction of oceanic lithosphere to that of continental lithosphere, prior to the development of the intensely studied NE-directed Apennine foreland fold and thrust belt.

Acknowledgements

Thorough review by Agustin Martin-Algarra and useful comments by JG Editor Randell Stephenson allowed us to substantially improve the paper. We are grateful to Glauco Bonardi for the innumerable and invaluable discussions.

6.1 References

Amore, O., Bonardi, G., Ciampo, G., De Capoa, P., Perrone, V., Sgrosso, I., 1988. Relazioni tra "flysch interni" e domini appenninici: reinterpretazione delle formazioni di Pollica, San

Mauro e Albidona e il problema dell'evoluzione inframiocenica delle zone esterne appenniniche. Mem. Soc. Geol. It., 41, 285-299.

Bonardi, G., Amore, F.O., Ciampo, G., de Capoa, P., Miconnet, P., Perrone, V., 1988. Il Complesso Liguride Auct.: stato delle conoscenze e problemi aperti sulla sua evoluzione pre-appenninca ed i suoi rapporti con l'arco calabro. Mem. Soc. Geol. It., 41, 17-35.

Bonardi, G., Cavazza, W., Perrone, V., Rossi, S., 2001. Calabria-Peloritani terrane and northern Ionian Sea. In: G.B. Vai & I.P. Martini (eds.), Anatomy of an Orogen: the Apennines and Adjacent Mediterranean Basins. Kluwer Academic Publishers, 287-306.

Bonardi, G., Caggianelli, A, Critelli, S., Messina, A., Perrone, V., Acquafredda, P., Carbone, G., Careri, G., Cirrincione, R., D'errico, M., Dominici, R., Festa, V., Iannace, A., Macaione, E., Mazzoli, S., Notaro, P., Parente, M., Perri, E., Piluso, E., Somma, R., Sonnino, M., Vitale, S., 2004. Geotraverse across the Calabria-Peloritani Terrane (southern Italy). Field Trip Guide Books vol. VI. Memorie Descrittive della Carta Geologica D'Italia, 63, 1-60.

Bonardi, G., Ciarcia, S., Di Nocera, S., Matano, F., Sgrosso, I., Torre, M., 2009. Carta delle principali Unità Cinematiche dell'Appennino meridionale. Boll. Soc. Geol. It., 128, Tav. f. t.

Cammarosano, A., Danna, M., De Rienzo, F., Martelli, L., Miele, F. , Nardi, G., 2000. Il substrato del Gruppo del Cilento tra il M. Vesalo e il M. Sacro (Cilento, Appennino Meridionale). Boll. Soc. Geol. It., 119, 395-405.

Cammarosano, A., Cavuoto, G., Danna, M., de Capoa, P., de Rienzo, F., Di Staso, A., Giardino, S., Martelli, L., Nardi, G., Sgrosso, A., Toccaceli, R.M., Valente, A., 2004. Nuovi dati sui flysch del Cilento (Appennino meridionale, Italia). Boll. Soc. Geol. It., 123, 253-273.

Ciarcia, S., Vitale, S., Di Staso, A., Iannace, A., Mazzoli, S., Torre, M., 2009. Stratigraphy and tectonics of an Internal Unit of the southern Apennines: implications for the geodynamic evolution of the peri-Tyrrhenian mountain belt. Terra Nova, 21, 88-96.

Donzelli, G., Crescenti, U., 1962. Lembi di Flysch oligocenico affiorante a SE della Piana del Sele. Mem. Soc. Geol. It., 3, 569-592.

496 Ghezzi, G., Bayliss, D.D., 1964. Uno studio del flysch nella regione calabro-lucana.
497 Stratigrafia, tettonica e nuove idee sul Miocene dell'Appennino meridionale. Boll. Serv. Geol.
498 d'It., 84, 3-64

499 Guerrera, F., Martín-Martín, M., Perrone, V., Tramontana, M., 2005. Tectono-sedimentary
500 evolution of the southern branch of the Western Tethys (Maghrebian Flysch Basin and
501 Lucanian Ocean): consequences for Western Mediterranean geodynamics. Terra Nova, 17,
502 358–367.

503 Iannace, A., Vitale, S., D'errico, M., Mazzoli, S., Di Staso, A., Macaione, E., Messina, A.,
504 Reddy, S.M., Somma, R., Zamparelli, V., Zattin, M., Bonardi, G. 2007. The carbonate
505 tectonic units of northern Calabria (Italy): A record of Apulian paleomargin evolution and
506 Miocene convergence, continental crust subduction, and exhumation of HP-LT rocks. Journal
507 of Geological Society, 164, 1165-1186.

508 Ietto, A., Pescatore, T., Cocco, E., 1965. Il flysch mesozoico-terziario del Cilento occidentale.
509 Boll. Soc. Natur. Napoli, 74, 396-402.

510 Johnston, S.T., Mazzoli, S., 2009. The Calabrian Orocline: buckling of a previously more
511 linear orogen. In: Murphy, J.B., Keppie, J.D., Hynes, A.J., (Eds.). Ancient Orogens and
512 Modern Analogues. Geological Society, London, Special Publications, 327, 113-125, doi:
513 10.1144/SP327.7 0305-8719/09/$15.00.

514 Mazzoli, S., Helman, M., 1994. Neogene patterns of relative plate motion for Africa–Europe:
515 some implications for recent central Mediterranean tectonics. Geologische Rundschau, 83,
516 464-468.

517 Mazzoli, S., D'Errico, M., Aldega, L., Corrado, S., Invernizzi ,C., Shiner, P., Zattin, M. 2008.
518 Tectonic burial and 'young' (< 10 Ma) exhumation in the southern Apennines fold and thrust
519 belt (Italy). Geology, 36, 243-246, doi: 10.1130/G24344A.

520 Mostardini, F., Merlini, S., 1986. Appennino centro meridionale. Sezioni geologiche e
521 proposta di modello strutturale. Mem. Soc. Geol. It., 35, 177-202.

522 Pescatore, T., Sgrosso, I., Torre, M., 1970. Lineamenti di tettonica e sedimentazione nel
523 Miocene dell'Appennino campano-lucano. Mem. Soc. Nat. in Napoli, 78, 337-408.
524 Price, N.J., Cosgrove, J.W., 1990. Analysis of geological structures. Cambridge University
525 Press, Cambridge.
526 Ramsay, J.G., 1967. Folding and fracturing of rocks. McGraw Hill: Book Company, New
527 York.
528 Ramsay, J.G., Huber, M., 1983. The Techniques of Modern Structural Geology. Volume I:
529 Strain Analysis. Academic Press, London.
530 Ranalli, G., Pellegrini, R., D'Offizi, S., 2000. Time dependence of negative buoyancy and the
531 subduction of continental lithosphere, J. Geodyn., 30, 539-555.
532 Russo, M., Zuppetta, A., Guida, A., 1995. Alcune precisazioni stratigrafiche sul Flysch del
533 Cilento (Appennino meridionale). Boll. Soc. Geol. It., 114, 353-359.
534 Selli, R., 1962. Il Paleogene nel quadro della geologia dell'Italia meridionale. Mem. Soc.
535 Geol. It., 3, 737-790.
536 Schettino, A., Turco, E., 2006. Plate kinematics of the Western Mediterranean region during
537 the Oligocene and Early Miocene. Geophys. J. Int., 166, 1398-1423.
538 Vignaroli, G., Faccenna, C., Rossetti, F., Jolivet, L., 2009. Insights from the Apennines
539 metamorphic complexes and their bearing on the kinematics evolution of the orogen. In:, Van
540 Hinsbergen, D.J.J., Edwards, M.A., Govers, R. (Eds.), Collision and Collapse at the Africa-
541 Arabia-Eurasia Subduction Zone. The Geological Society, London, Special Publications, 311,
542 235-256.
543 Vitale, S. Mazzoli S., 2009. Finite strain analysis of a natural ductile shear zone in limestones:
544 insights into 3-D coaxial vs. non-coaxial deformation partitioning. Journal of Structural
545 Geology, 31, 104-113, doi: 10.1016/j.jsg.2008.10.011.
546 Vitale, S., Ciarcia, S., Mazzoli, S., Iannace, A., Torre, M., 2010. Structural analysis of an
547 Internal Unit of the southern Apennines (Cilento area, Italy): new constraints on the

548 geodynamic evolution of the Miocene Apennine accretionary wedge. Comptes Rendus
549 Geosciences, doi: 10.1016/j.crte.2010.03.005.
550 Zuppetta, A., Mazzoli, S., 1997. Deformation history of a synorogenic sedimentary wedge,
551 northern Cilento area southern Apennines thrust and fold belt, Italy. Geological Society of
552 America Bulletin, 109, 698-708.

553

554 Figure captions

555

556 Fig. 1. Tectonic sketch map of the southern Apennines (after Bonardi et al., 2009, modified).
557 Inset shows thrust front of the peri-Tyrrhenian mountain belt.

558

559 Fig. 2. Sketch showing tectonic and stratigraphic relationships between Liguride Units and
560 Miocene wedge-top basin deposits.

561

562 Fig. 3. (a) Geological sketch map of the Cilento area, showing all analyzed outcrop locations;
563 (b) Geological cross-sections (located in a).

564

565 Fig. 4. Sketch showing stratigraphic relationships for the Nord-Calabrese and Parasicilide
566 Units, the Cilento Group and the Monte Sacro Fm.

567

568 Fig. 5. Examples of outcrop features in the Crete Nere Fm (a) and in the lower part of the
569 Saraceno Fm (b) to (h). (a) Interference pattern between isoclinal F_1^{NC} and close F_2^{NC} folds
570 (Torre di Caleo-Pioppi). (b) Interference pattern between isoclinal F_1^{NC} and open F_2^{NC} folds
571 (Punta Telegrafo). (c) Crenulation cleavage (S_2^{NC}) deforming preexisting pervasive foliation

572 (S_1^{NC}) (Punta Telegrafo). (d) F_2^{NC} folds (Punta Telegrafo). (e) Bedding-parallel shear zone
573 consisting of rotated calcareous clasts embedded in foliated pelite (formed by disruption of
574 pre-existing limestone-shale alternations; Pioppi). (f) Chocolate tablet boudinage in
575 calcareous bed (Punta Telegrafo). (g) Rotated boudin (detail of en echelon boudin structure)
576 in calcareous layer embedded in pelite (Torre di Caleo). (h) Shortened boudinage (Torre di
577 Caleo).
578
579 Fig. 6. Lower hemisphere, equal-area projections showing orientation data for measured
580 structures in the Crete Nere Fm.
581
582 Fig. 7. Lower hemisphere, equal-area projections showing orientation data for measured
583 structures in the Saraceno Fm.
584
585 Fig. 8. Examples of outcrop features in the Saraceno and Pollica Fms. Interference between
586 isoclinal F_1^{NC} folds and close F_2^{NC} folds, middle part of the Saraceno Fm: (a) Torre di Caleo; (b)
587 Ascea-Pisciotta. (c) F_1^{CG} detachment fold in the Cannicchio Sandstones Member, showing
588 (boxed) accommodation thrusts in thin arenite layer located in the fold hinge region
589 (Cannicchio). (d) Pre-buckle thrust in the Cannicchio Sandstones Member (Cannicchio). (e)
590 Kink fold in the middle part of the Pollica Fm (Agnone). (f) Brecciated sandstone in the hinge
591 region of F_1^{CG} fold, middle part of the Pollica Fm (Ogliastro Marina). (g)-(h)-(i) Pre-buckle
592 thrusts in competent beds of the middle part of the Pollica Fm (Ogliastro).
593
594 Fig. 9. Lower hemisphere, equal-area projections showing orientation data for measured
595 structures in the Pollica and San Mauro Fms.

596

597 Fig. 10. Tectonic model showing present-day geometric relationships among the studied
598 units.

599

600 Fig. 11. Sketch showing the reconstructed geodynamic evolution of the Cilento accretionary
601 wedge between the Aquitanian and the early Tortonian.

602

603 Table caption

604

605 Table 1. Correlation among deformation stages for the studied successions and related
606 chronology.

607

Figure01

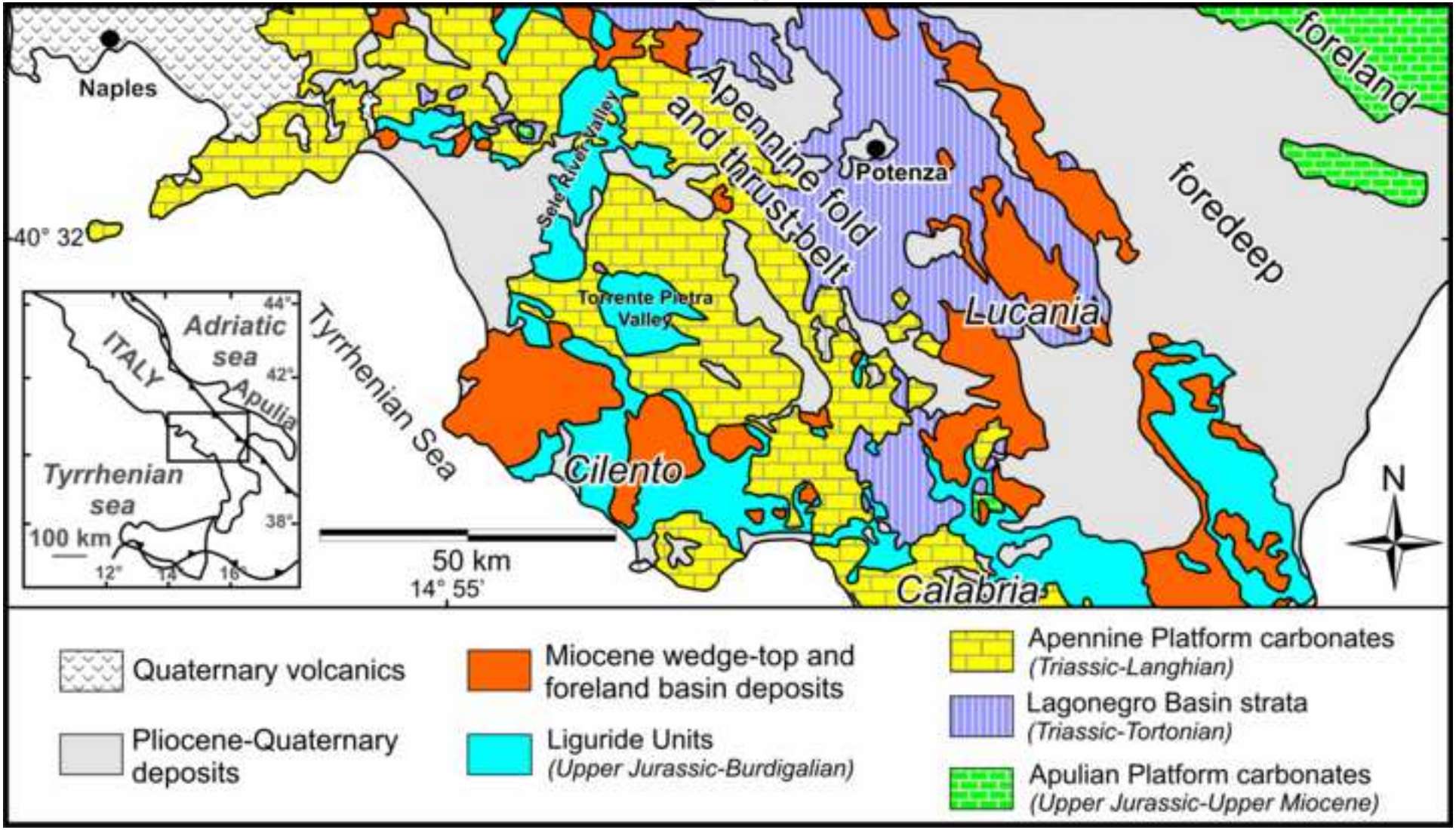
Naples
Potenza
Sele River Valley
Apennine fold and thrust-belt
foreland
foredeep
40° 32
Torrente Pietra Valley
Lucania
Tyrrhenian Sea
Cilento
Calabria
N
50 km
14° 55'
ITALY
Adriatic sea
Apulia
Tyrrhenian sea
100 km
44°
42°
38°
12°
14°
16°
Quaternary volcanics
Pliocene-Quaternary deposits
Miocene wedge-top and foreland basin deposits
Liguride Units
(Upper Jurassic-Burdigalian)
Apennine Platform carbonates
(Triassic-Langhian)
Lagonegro Basin strata
(Triassic-Tortonian)
Apulian Platform carbonates
(Upper Jurassic-Upper Miocene)

Figure02

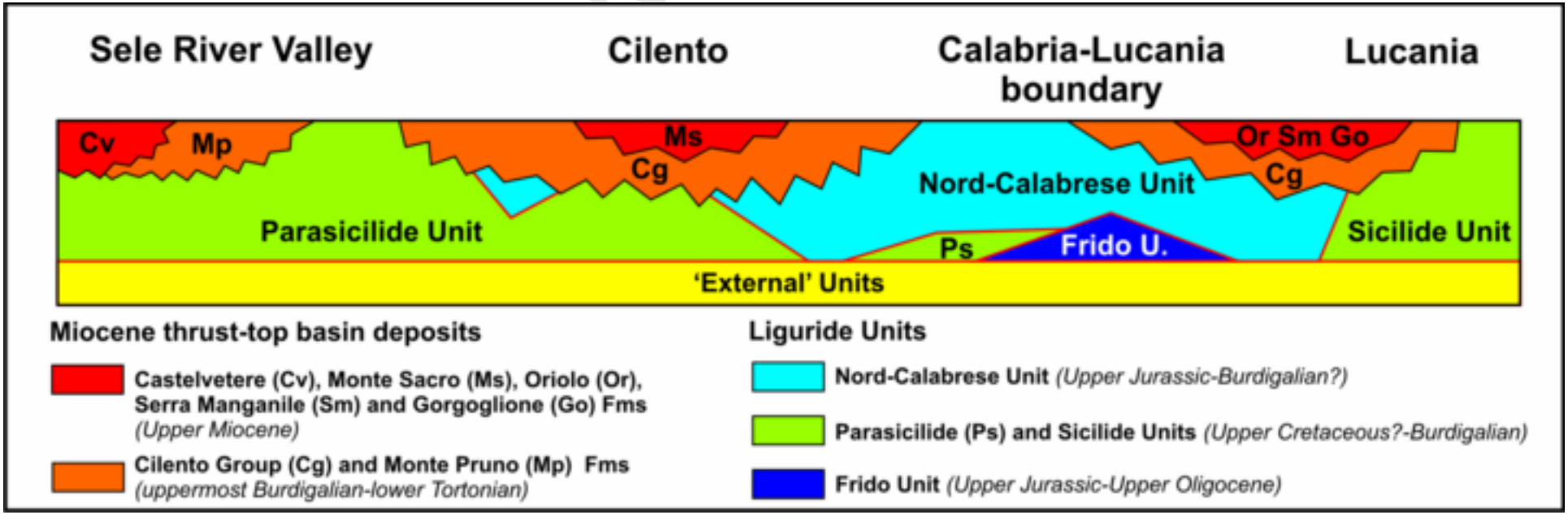

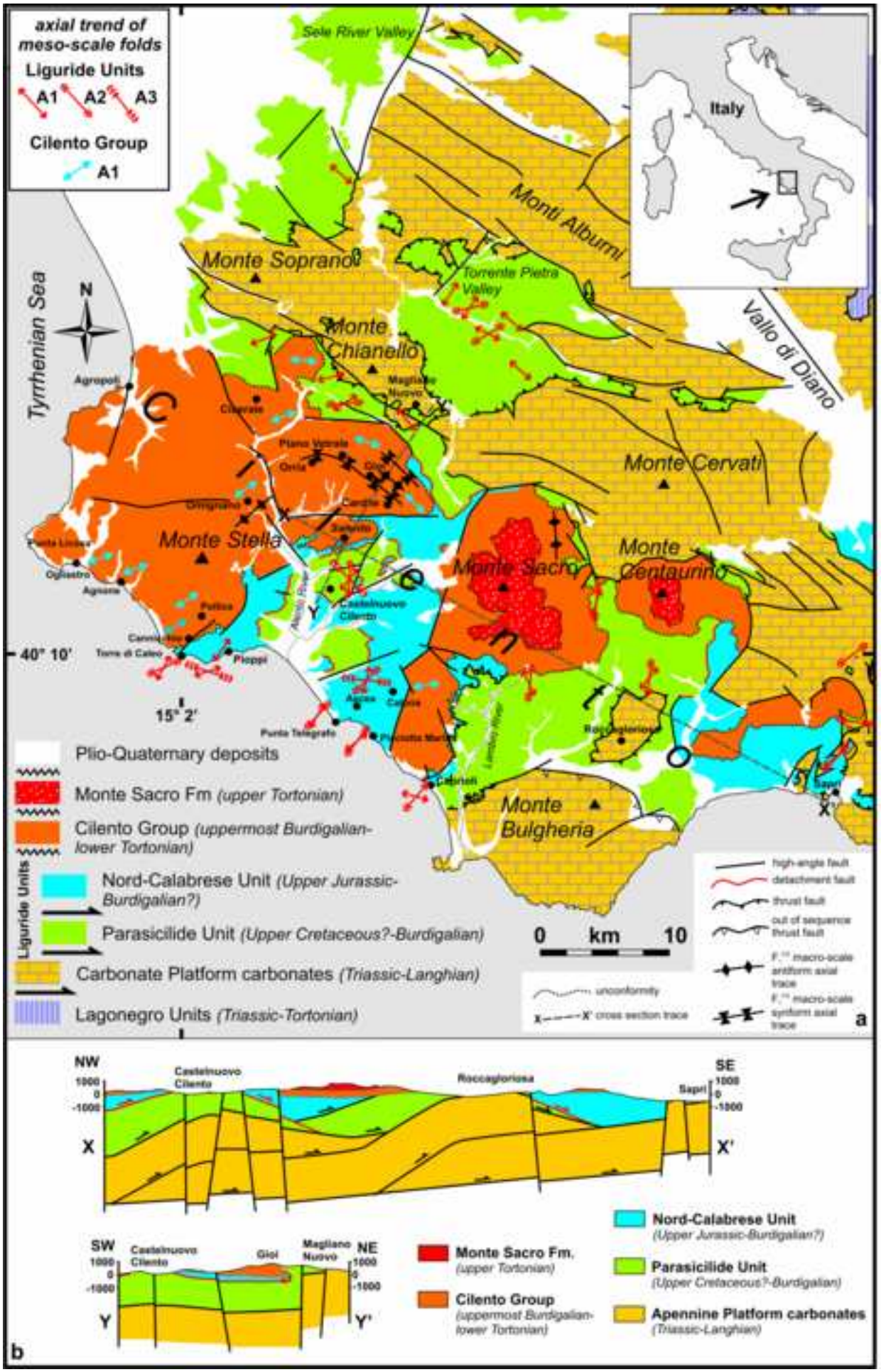

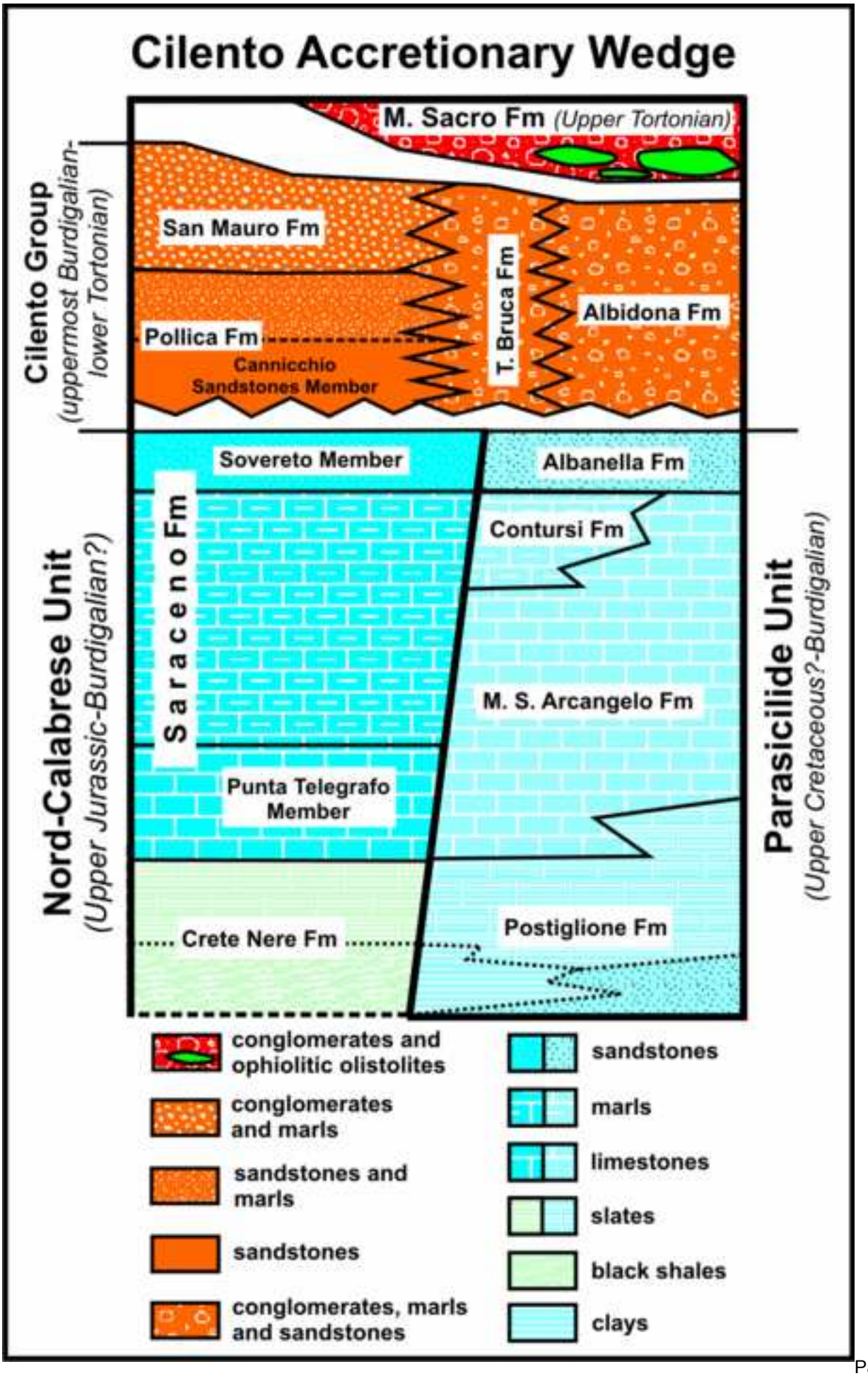

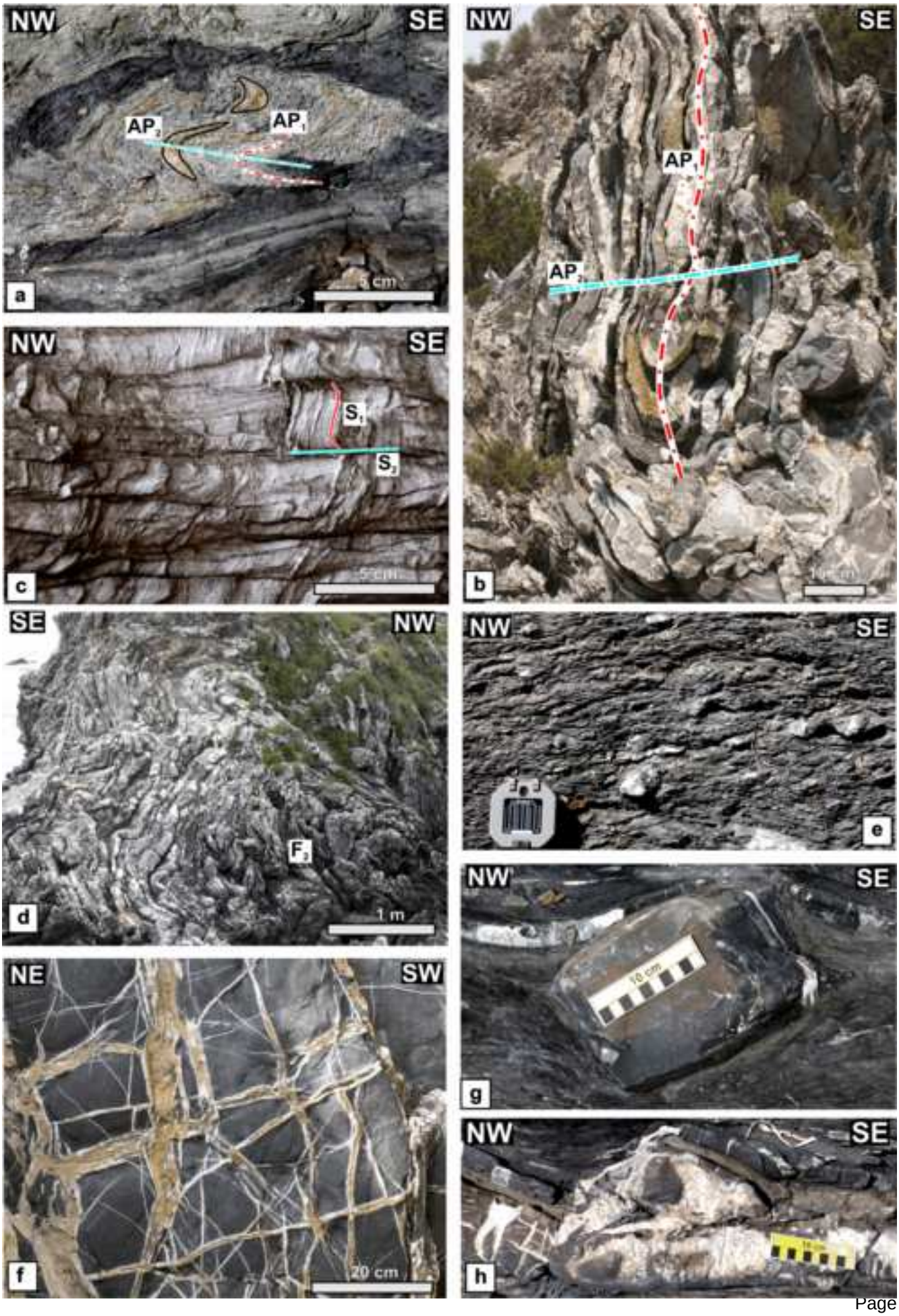

Figure06

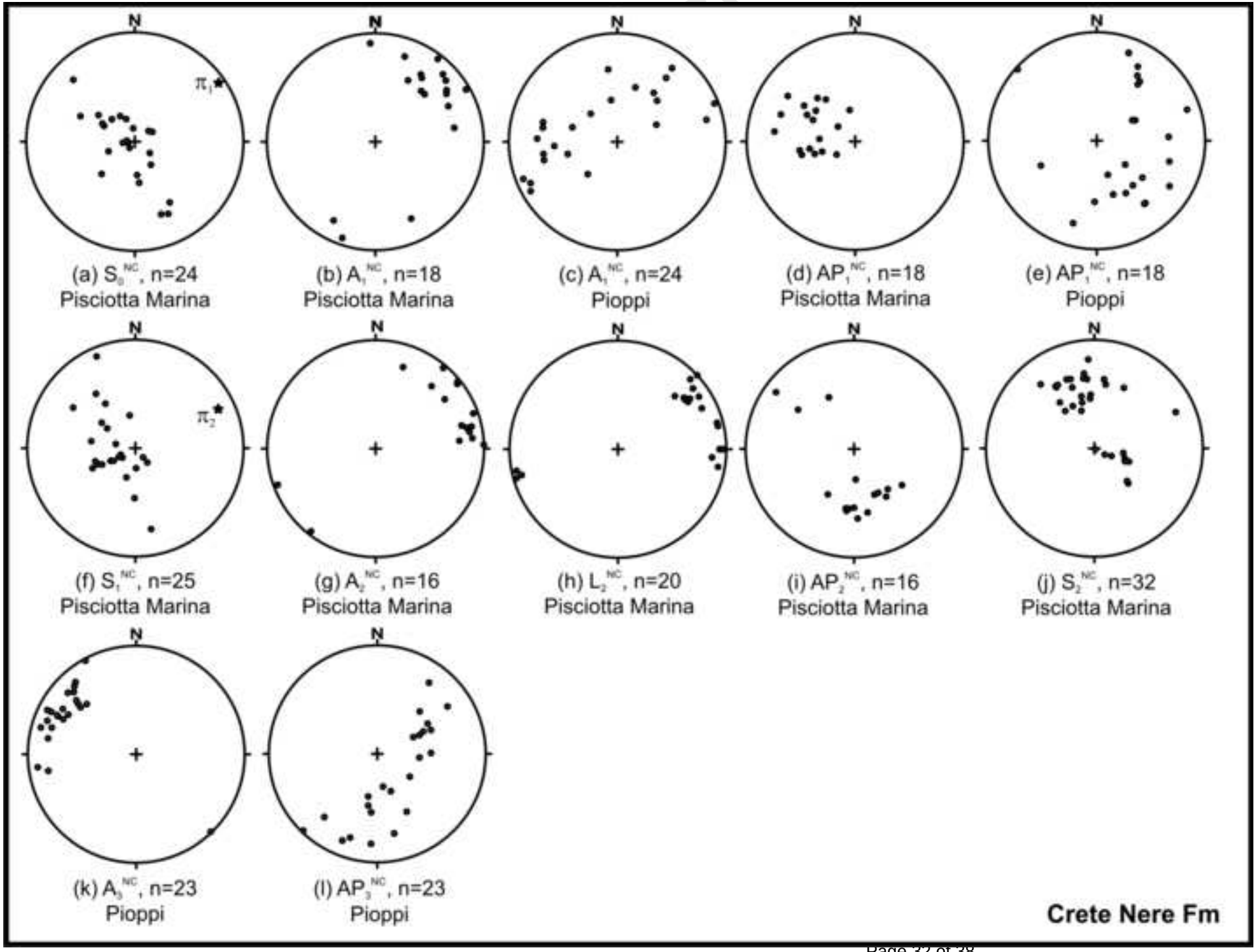
N
π1
(a) S0NC, n=24
Pisciotta Marina
(b) A1NC, n=18
Pisciotta Marina
(c) A1NC, n=24
Pioppi
(d) AP1NC, n=18
Pisciotta Marina
(e) AP1NC, n=18
Pioppi
π2
(f) S1NC, n=25
Pisciotta Marina
(g) A2NC, n=16
Pisciotta Marina
(h) L2NC, n=20
Pisciotta Marina
(i) AP2NC, n=16
Pisciotta Marina
(j) S2NC, n=32
Pisciotta Marina
(k) A3NC, n=23
Pioppi
(l) AP3NC, n=23
Pioppi
Crete Nere Fm

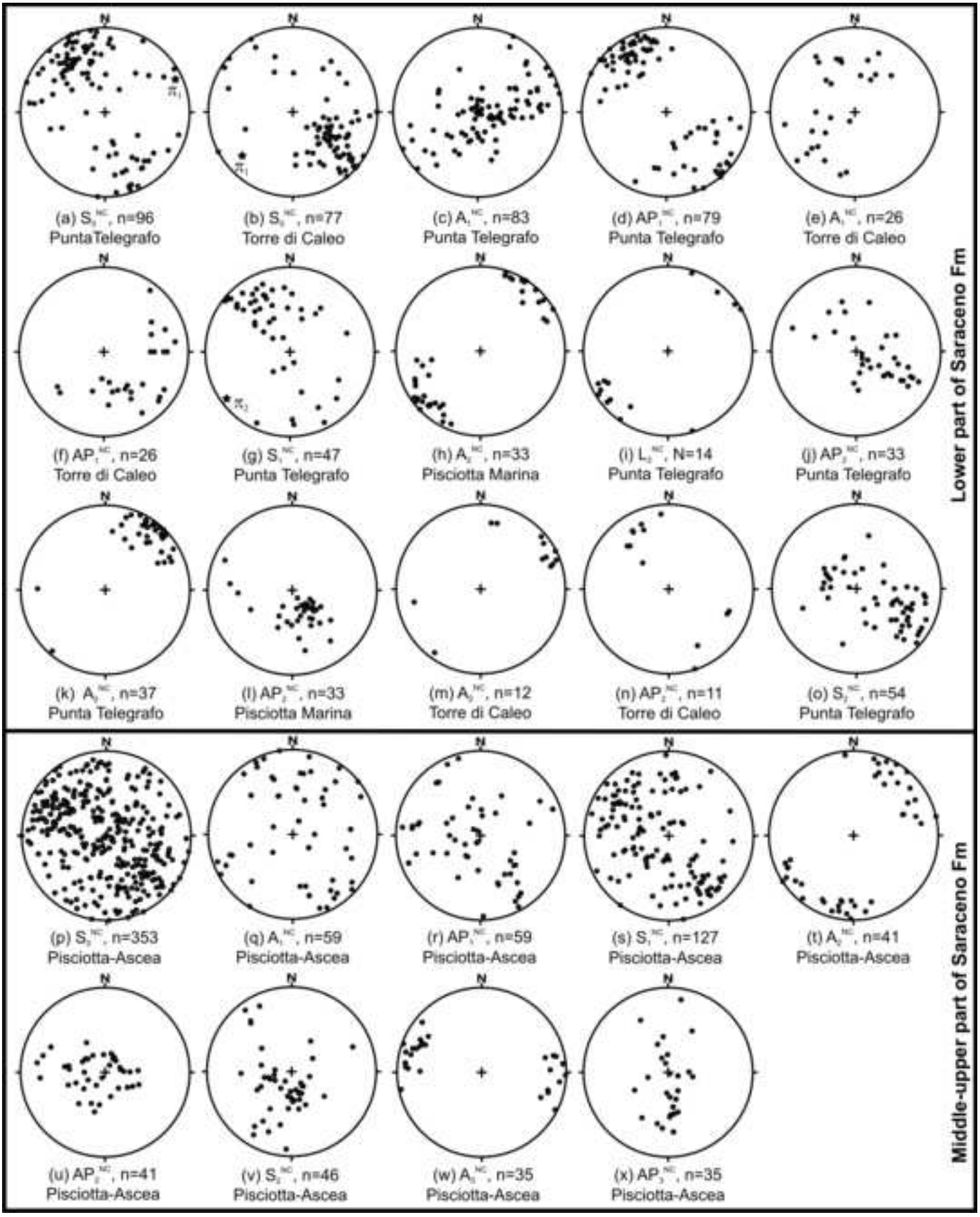

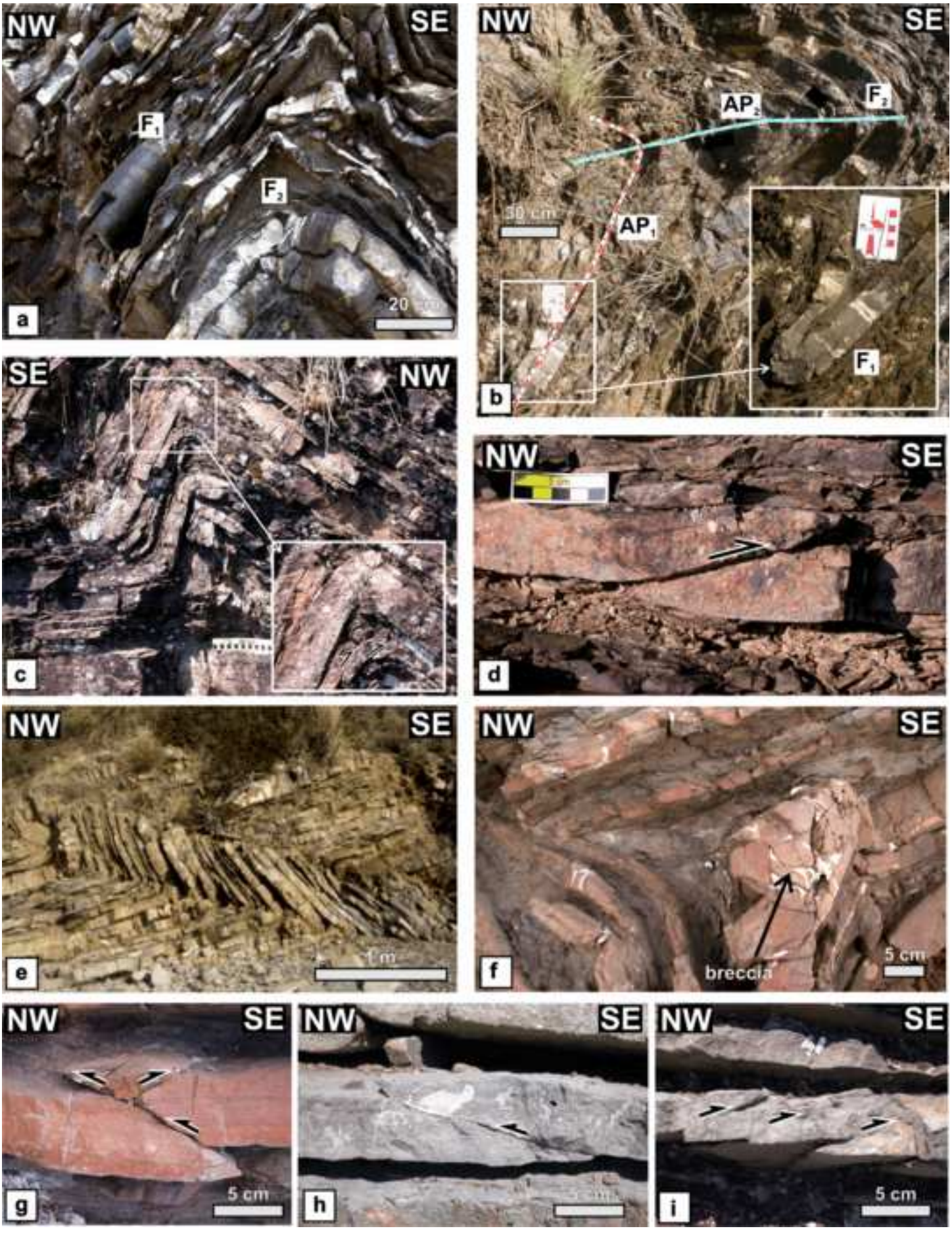

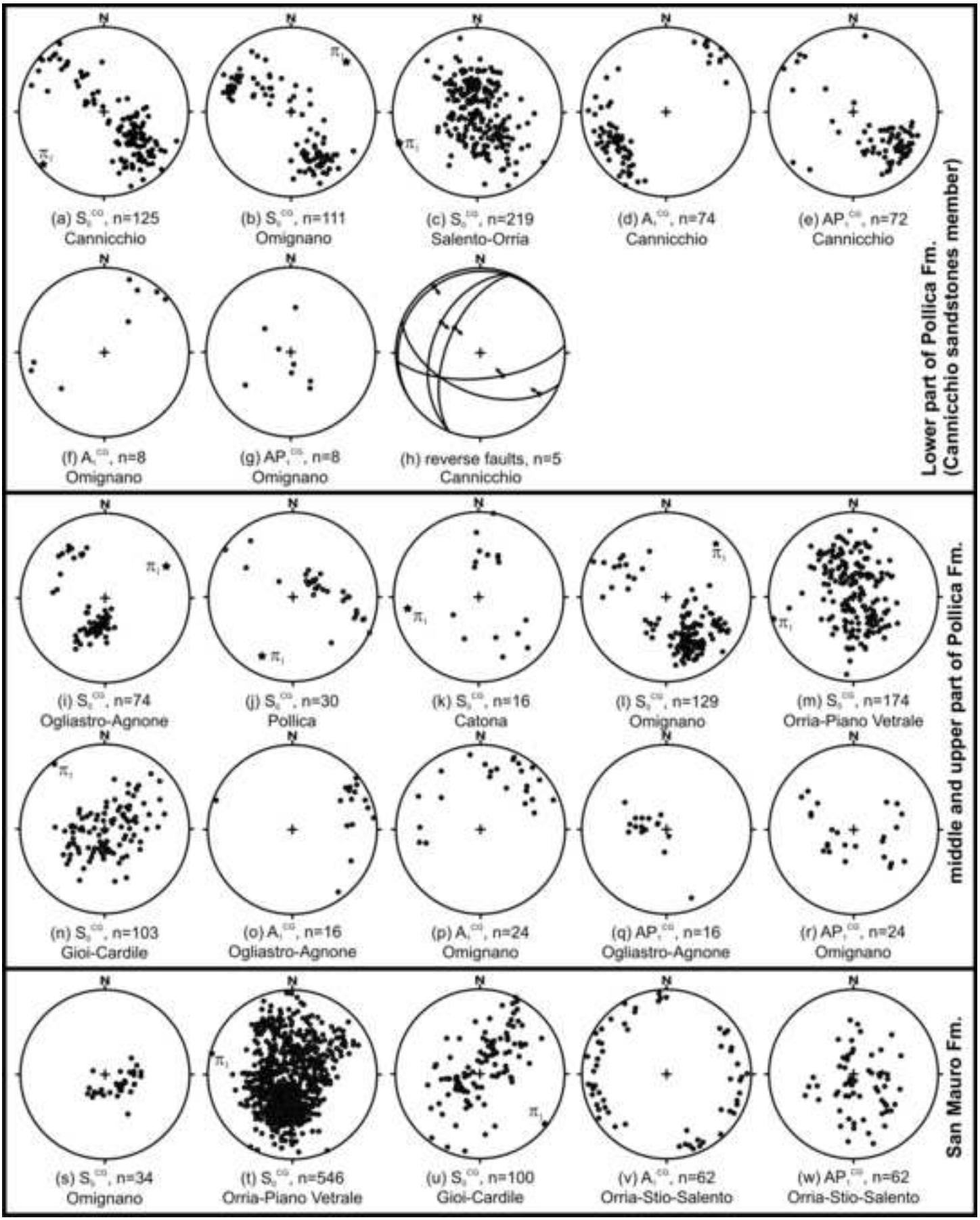

Figure10

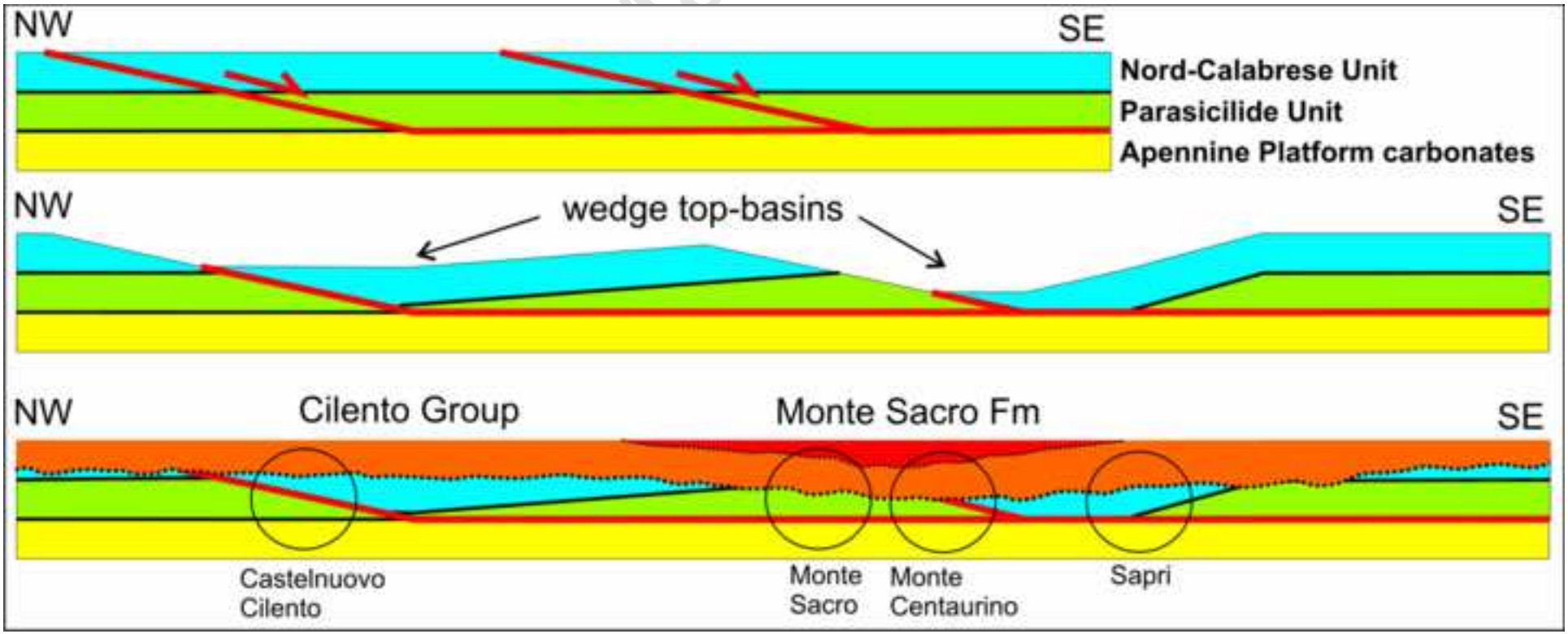
NW
SE
Nord-Calabrese Unit
Parasicilide Unit
Apennine Platform carbonates
NW
wedge top-basins
SE
NW
Cilento Group
Monte Sacro Fm
SE
Castelnuovo Cilento
Monte Sacro
Monte Centaurino
Sapri

Figure11

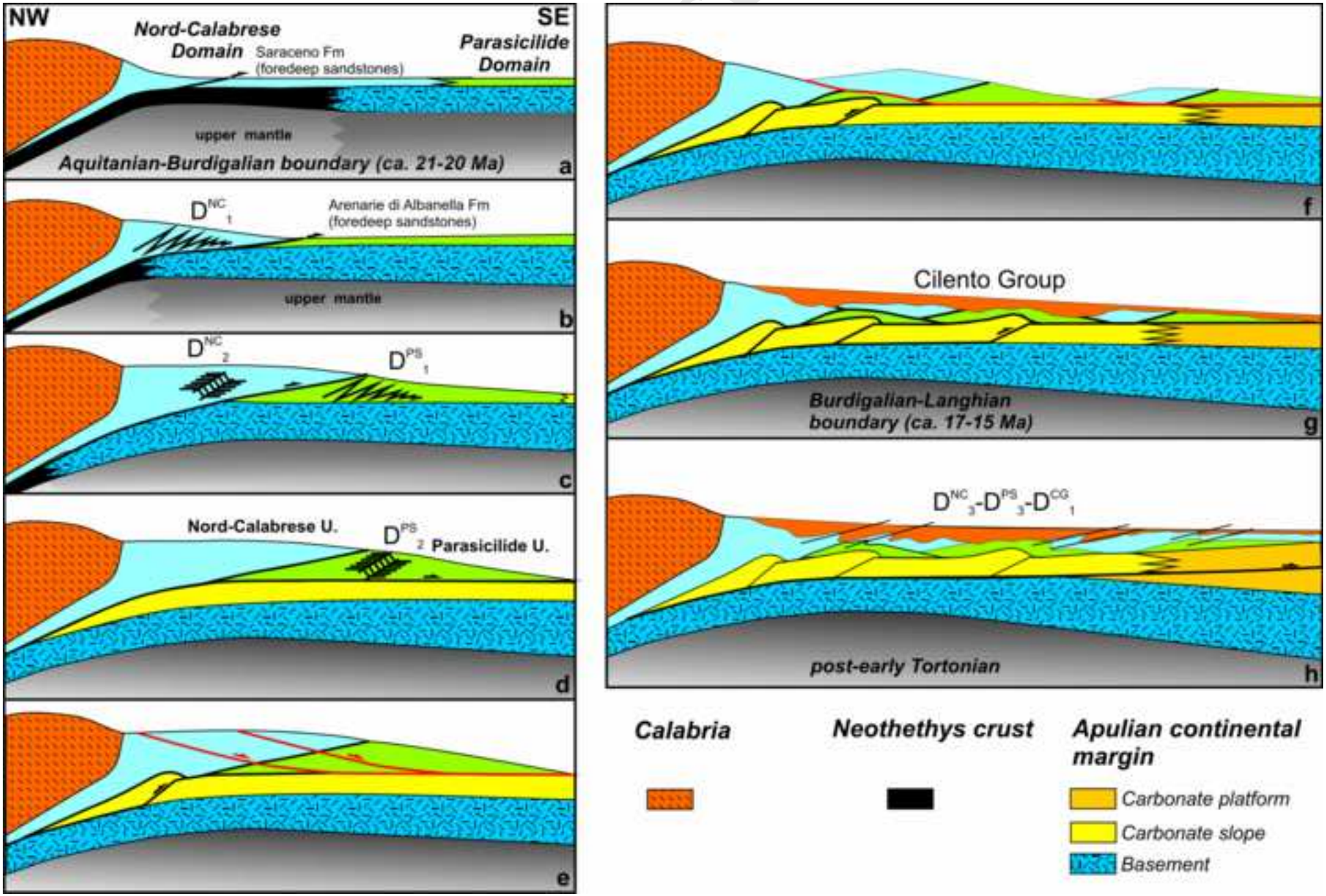
NW
SE
Nord-Calabrese Domain
Saraceno Fm (foredeep sandstones)
Parasicilide Domain
upper mantle
Aquitanian-Burdigalian boundary (ca. 21-20 Ma)
a
D^{NC}_{1}
Arenarie di Albanella Fm (foredeep sandstones)
upper mantle
b
D^{NC}_{2}
D^{PS}_{1}
c
Nord-Calabrese U.
D^{PS}_{2}
Parasicilide U.
d
e
f
Cilento Group
Burdigalian-Langhian boundary (ca. 17-15 Ma)
g
D^{NC}_{3}-D^{PS}_{3}-D^{CG}_{1}
post-early Tortonian
h
Calabria
Neothethys crust
Apulian continental margin
Carbonate platform
Carbonate slope
Basement

	Burdigalian			early Tortonian
	I	II	III	
Cilento Group				D^{CG}_{1}
Parasicilide Unit		D^{PS}_{1}	D^{PS}_{2}	D^{PS}_{3}
Nord-Calabrese Unit	D^{NC}_{1}	D^{NC}_{2}		D^{NC}_{3}